Journal of Catalysis **186,** 254–268 (1999)
Article ID jcat.1999.2558, available online at http://www.idealibrary.com on IDEAL®

Selective Catalytic Reduction of Nitrogen Oxides by Ammonia over Fe^{3+}-Exchanged TiO_2-Pillared Clay Catalysts

R. Q. Long and R. T. Yang[1]

Department of Chemical Engineering, University of Michigan, Ann Arbor, Michigan 48109-2136

Received November 24, 1998; revised May 12, 1999; accepted May 14, 1999

Fe-exchanged TiO_2-pillared clay (PILC) catalysts were prepared and used for selective catalytic reduction (SCR) of NO_x by ammonia. They were also characterized for surface area, pore size distribution, and by XRD, H_2-TPR, and FT-IR methods. The Fe–TiO_2–PILC catalysts showed high activities in the reduction of NO_x by NH_3 in the presence of excess oxygen. SO_2 further increased the catalytic activities at above 350°C, whereas H_2O decreased the activity slightly. The catalysts were about twice as active as commercial-type V_2O_5–WO_3/TiO_2 catalyst in the presence of H_2O and SO_2. Moreover, compared to the commercial catalyst, the Fe–TiO_2–PILC catalysts had higher N_2/N_2O product selectivities (e.g., 0–1% vs 9% N_2O at 400°C) and substantially lower activities (by 74–88%) for SO_2 oxidation to SO_3 under the same reaction conditions. The activity was further increased to over three times that of the vanadia-based catalyst when Ce was added. The high activity and low N_2O selectivity for the Fe–TiO_2–PILC catalysts were attributed to their low activity in the oxidation of ammonia, as compared with vanadia catalysts. XRD patterns of Fe–TiO_2–PILC were similar to those of TiO_2–PILC, showing no peaks due to iron oxide, even when the iron content reached 20.1%. The TPR results indicated that iron in the Fe–TiO_2–PILC catalysts with lower iron contents existed in the form of isolated Fe^{3+} ions. The activities of Fe–TiO_2–PILC catalysts were consistent with their surface acidities, which were identified by FT-IR of the NH_3-adsorbed samples. The enhancement of activities by $H_2O + SO_2$ was attributed to the increase of surface acidity resulting from the formation of surface sulfate species of iron.

Key Words: **selective catalytic reduction; SCR by NH_3, Fe–TiO_2–PILC; pillared clay; pillared clay catalyst for NO reduction.**

INTRODUCTION

Nitrogen oxides (NO_x, $x = 1, 2$) resulting from combustion are a major source of air pollution. The major technology for reducing NO emissions from stationary sources is selective catalytic reduction (SCR) of NO_x with ammonia, forming nitrogen and water. In the SCR reaction, catalysts of different compositions have been used (1). The commercial catalysts that are used today are V_2O_5 mixed with WO_3 and/or MoO_3 supported on TiO_2. Although the vanadium-based catalysts are highly active, major disadvantages remain, such as their toxicity and high activity for the oxidation of SO_2 to SO_3. The SO_3 combines with NH_3 and H_2O and results in the formation of NH_4HSO_4, $(NH_4)_2S_2O_7$, and H_2SO_4, which cause corrosion and plugging of equipment. The significant selectivity for forming N_2O is another disadvantage of the V_2O_5 based catalysts. Hence there are continuing efforts for developing new catalysts (1).

In addition to V_2O_5, a large number of other catalysts, such as those containing Fe, Cr, Cu, or Ni oxides, also have high activities for the SCR reaction. Iron-based catalysts are particularly attractive because of their high activity, low cost, and lack of toxicity as compared to V_2O_5/TiO_2 catalysts. Okazaki *et al.* (2) reported that pure iron oxide showed only a moderate activity, but mixing 5% $Nb_2O_5 \cdot xH_2O$ to Fe_2O_3 significantly increased the activity. The promoting effect by $Nb_2O_5 \cdot xH_2O$ was attributed to an increase in acidity (3). Nobe and co-workers also reported that addition of small amounts of V_2O_5 and/or Cr_2O_3 to Fe_2O_3/TiO_2 and Fe_2O_3/Al_2O_3 improved their activities (4, 5). In particular, a ratio of $Fe/Cr = 9$ yielded the highest NO_x conversion (4). However, the catalytic activities of the above Fe_2O_3-based catalysts were lower than those of the V_2O_5-based catalysts (5). Recently, we have found that high SCR activities, much higher than Fe_2O_3/Al_2O_3 and Fe_2O_3/TiO_2, were obtained on Fe_2O_3-pillared clays and Fe_2O_3/Cr_2O_3 (3/1) doped TiO_2-pillared clays (6, 7). The activity of the latter was also substantially higher than that of the commercial V_2O_5–WO_3/TiO_2 catalyst (7).

Pillared interlayer clays (PILCs), or pillared clays, are two-dimensional layer materials prepared by exchanging the charge-compensating cations between the clay layers with larger inorganic hydroxyl metal cations formed by hydrolysis of metal salts. Upon heating, the metal hydroxyl cations undergo dehydration and dehydroxylation, forming stable metal oxide clusters which act as pillars keeping the silicate layers separated and creating interlayer spacing (gallery) of molecular dimension. Both Lewis and Brønsted acid sites exist on pillared clays. The acidity and acid site types (Brønsted or Lewis) depend on the

[1] Corresponding author. E-mail: yang@umich.edu.

0021-9517/99 $30.00

exchanged cations, preparation method, and starting clay (8–10). PILCs have been studied as catalysts in some acid-catalyzed reactions, e.g., fluid catalytic cracking, alcohol dehydration, and alkylation (9, 10). It is known that surface acidity is very important for the SCR reaction of NO_x by NH_3 (6, 7, 11–13). PILCs, metal oxide doped PILCs and ion exchanged PILCs were synthesized and tested for their activities for SCR in our previous studies (14, 15). It was found that the activity decreased in the order Cr_2O_3–PILC > Fe_2O_3–PILC > TiO_2–PILC > ZrO_2–PILC > Al_2O_3–PILC, and Cr_2O_3–PILC exhibited higher activities than V_2O_5–WO_3/TiO_2 catalyst, but its activity was severely decreased by SO_2 (15).

In this study, a substantial improvement on the SCR activity is achieved on iron ion-exchanged TiO_2–PILC. The reason for choosing TiO_2–PILC is that TiO_2–PILC has the following desirable characteristics: (a) high thermal and hydrothermal stability among all the pillared clays as demonstrated by TGA results (16), (b) large pore sizes that allow further incorporation of active ingredients without hindering pore diffusion (7, 9, 14), (c) intercalating TiO_2 between the SiO_2 tetrahedral layers is a unique way of increasing surface area and acidity of the TiO_2 support (7, 14), and (d) titania-based SCR catalysts have been found to be highly resistant to SO_2 poisoning and also possess durability (7, 14, 17). It is found that the Fe-exchanged TiO_2–PILC catalysts showed higher activities and N_2/N_2O product selectivities for NO_x reduction, but lower activities for SO_2 oxidation to SO_3, as compared with the commercial-type V_2O_5–WO_3/TiO_2 catalyst. Particularly, the catalytic activities are increased by H_2O and SO_2, which is attributed to the increase of the surface acidity of the catalysts.

EXPERIMENTAL

Catalyst Preparation

TiO_2–PILC was synthesized by following established procedures (7, 18). The starting clay was a purified montmorillonite, i.e., a purified-grade bentonite powder from Fisher Company, with particles of size less than or equal to 2 μm. The bentonite has the following compositions: 60.3% SiO_2, 19.1% Al_2O_3, 3.7% Fe_2O_3, 0.2% TiO_2, 1.4% CaO, 2.4% MgO, 2.9% Na_2O, and 0.5% K_2O. The cation exchange capacity (CEC) of the clay was 103 meq/100 g. The pillaring agent, a solution of partially hydrolyzed Ti-polycations, was prepared by first adding $TiCl_4$ into a 2 M HCl solution. The mixture was then diluted by slowly adding deionized water with constant stirring to reach a final Ti concentration of 0.82 M. The final concentration of HCl was 0.6 M. The solution was aged for more than 8 h at room temperature prior to its use. Eight grams bentonite was dispersed in 2.0 L deionized water and the slurry was stirred for 5 h. The pillaring solution was slowly added into the suspension of clay with vigorous stirring until the amount of pillaring solution reached that required to obtain a 10 mmol Ti/g clay. The resulting product was left in contact with the solution for 18 h. Subsequently, the clay particles were separated by vacuum filtration and washed with deionized water until the washing liquid was free of chloride ions as indicated by using silver nitrate test. The sample was dried at 120°C for 12 h and then calcined at 350°C for 12 h.

TABLE 1

Preparation Conditions and Iron Contents of the Fe–TiO_2–PILC Catalysts

Sample	Fe content (wt%)	Preparation conditions
TiO_2–PILC	1.53	—
Fe(4)–TiO_2–PILC	4.32	Ion exchange 6 h at room temperature (once)
Fe(6)–TiO_2–PILC	5.93	Ion exchange 6 h at room temperature (twice)
Fe(8)–TiO_2–PILC	7.74	Ion exchange 6 h at 50°C (once)
Fe(20)–TiO_2–PILC	20.1	Ion exchange 6 h at 50°C (3 times)
Ce–Fe(5)–TiO_2–PILC	5.45	Ce exchange 20 h, then Fe exchange 6 h (twice) at room temperature

The iron ion-exchanged TiO_2–PILC catalysts were prepared by using a conventional ion exchange procedure. In each experiment, 2 g TiO_2–PILC was added to 200 ml 0.05 M $Fe(NO_3)_3$ solution with constant stirring. The pH value of the solution was 1.5. Four Fe–TiO_2–PILC samples under different ion exchange conditions were prepared and are summarized in Table 1. Ce–Fe–TiO_2–PILC catalysts were also prepared by exchanging TiO_2–PILC samples with 0.05 M $Ce(NO_3)_3$ solution for 20 h and then 0.05 M $Fe(NO_3)_3$ solution twice at room temperature; Ce exchange was done first because it was harder than ion-exchange for Fe^{3+}. The mixtures were filtered and washed five times with deionized water. The obtained solid samples were first dried at 120°C in air for 12 h, then calcined at 400°C for 6 h. Finally, the obtained samples were ground to 60–140 mesh. The iron contents obtained by neutron activation analysis in TiO_2–PILC, Fe(4)–TiO_2–PILC, Fe(6)–TiO_2–PILC, Fe(8)–TiO_2–PILC, Fe(20)–TiO_2–PILC, and Ce–Fe–TiO_2–PILC samples were 1.53 wt%, 4.32 wt%, 5.93 wt%, 7.74 wt%, 20.1 wt%, and 5.45 wt%, respectively (Table 1). The cerium content in Ce–Fe(5)–TiO_2–PILC was 0.51 wt%.

Besides pillared clay catalysts, V_2O_5–WO_3/TiO_2 catalyst (4.4% V_2O_5–8.2% WO_3/TiO_2) was also used for comparison. The catalyst was prepared by incipient wetness impregnation as described elsewhere (12). The V_2O_5–WO_3/TiO_2 catalyst had the same composition and surface area as a European commercial SCR catalyst as described by Tuenter *et al.* (19). Also, this catalyst had nearly identical SCR activity and behavior as that of the commercial SCR catalyst made by a major U.S. catalyst manufacturer (7).

Catalyst Characterization

Powder X-ray diffraction (XRD) was conducted with a Rigaku Rotaflex D/Max-C system with Cu $K\alpha$ ($\lambda = 0.1543$ nm) radiation. The samples were loaded on a sample holder with a depth of 1 mm. XRD patterns were recorded in the range $2\theta = 2$–45°.

A Micromeritics ASAP 2010 micropore size analyzer was used to measure the N_2 adsorption isotherms of the samples at liquid N_2 temperature (-196°C). The specific surface areas of the samples were determined from the linear portion of the BET plots ($P/P_0 = 0.05$–0.20). The pore size distribution was calculated from the desorption branch of the N_2 adsorption isotherm using the Barrett–Joyner–Halenda (BJH) formula, because the desorption branch can provide more information about the degree of blocking than the adsorption branch (20). Prior to the surface area and pore size distribution measurements, the samples were dehydrated at 350°C for 6 h.

In each H_2-TPR (temperature-programmed reduction) experiment, 0.1 g sample was loaded into a quartz reactor and then pretreated in a flow of He (40 ml/min) at 400°C for 0.5 h. After the sample was cooled down to room temperature in He, the reduction of the sample was carried out from 30 to 700°C in a flow of 5.34% H_2/N_2 (27 ml/min) at 10°C/min. The consumption of H_2 was monitored continuously with a thermal conductivity detector. The water produced during reduction was trapped in a 5A molecular sieve column.

Catalytic Activity Measurement

The SCR activity measurement was carried out in a fixed-bed quartz reactor. The reaction temperature was controlled by an Omega (CN-2010) programmable temperature controller. Either 0.2 or 0.1 g catalyst was used in this work. The flue gas was simulated by blending different gaseous reactants. Two sets of flow meters were used to control the flow rates of the individual reactants. He, NH_3/He, and NO/He gases were controlled by rotameters, whereas SO_2/He and O_2 were controlled by mass flow meters (FM 4575 Linde Division). The typical reactant gas composition was as follows: 1000 ppm NO, 1000 ppm NH_3, 2% O_2, 1000 ppm SO_2 (when used), 8% water vapor (when used), and balance He. The total flow rate was 500 ml/min (ambient conditions) and the GHSV (gas hourly space velocity) was 113 000 l/h or 226 000 l/h. The premixed gases (1.01% NO in He, 1.00% NH_3 in He, and 0.99% SO_2 in He) were supplied by Matheson. Water vapor was generated by passing He through a heated gas-wash bottle containing deionized water. The tubings of the reactor system were wrapped with heating tapes to prevent formation and deposition of ammonium sulfate/bisulfate and ammonium nitrate. The NO and NO_2 concentrations were continually monitored by a chemiluminescent NO/NO_x analyzer (Thermo Electro Corporation, Model 10). To avoid errors caused by the oxidation of ammonia in the converter of the NO/NO_x analyzer, an ammonia trap containing phosphoric acid solution was installed before the sample inlet to the chemiluminescent analyzer. The products were also analyzed by a gas chromatograph (Shimadzu, 14A) at 50°C with a 5A molecular sieve column for N_2 and a Porapak Q column for N_2O. Hence the nitrogen balance and the product selectivities for N_2 and N_2O could be obtained. All the data were obtained after 5 min when the SCR reaction reached steady state.

SO_3 Analysis

To measure the amount of SO_3 from SO_2 oxidation during the SCR reaction, a conventional wet analysis method was adopted. With the same reactor used for measuring the catalyst SCR activity, the effluent was bubbled through a solution containing $BaCl_2$ and HCl. After 12–24 h runs at 375°C under the conditions of 1000 ppm NO, 1000 ppm NH_3, 2% O_2, 8% H_2O, 1000 ppm SO_2, and GHSV = 113000 l/h, SO_3 was quantitatively captured and precipitated as $BaSO_4$ by the $BaCl_2$ solution. Since a small amount of ammonium sulfates (resulting from reactions of SO_3, H_2O, and NH_3) might have been deposited on the tubings between the SCR reactor and the $BaCl_2$ solution, we washed the tubings with deionized water which was collected in the $BaCl_2$ solution after the reaction. The $BaSO_4$ precipitate was collected on an ashless filter paper which was burned along with the precipitate in a crucible, so the amount of the precipitate was accurately measured.

FT-IR Characterization

Infrared spectra were measured with a Nicolet Impact 400 FT-IR spectrometer with a TGS detector. Self-supporting wafers of 1.3 cm diameter were prepared by pressing 20 mg samples and were loaded into a high-temperature IR cell with BaF_2 windows. The wafers were treated at 450°C for 30 min in a flow of He (99.9998%, 100 ml/min) and then cooled down to room temperature. At each temperature, i.e., 25, 100, 200, 300, 350, and 400°C, the background spectrum of sample was recorded in He. Adsorption of NH_3 was performed at room temperature in a flow of 1.00% NH_3/He (100 ml/min) for 30 min followed by purging for 15 min with He. The sample was subsequently heated in a flow of He step by step. At each temperature, the spectrum was recorded by accumulating 100 scans at a spectral resolution of 4 cm^{-1}. The NH_3 adsorption on the samples pretreated with H_2O and SO_2 at a high temperature (400°C) was also studied in this work.

RESULTS

XRD Analysis

X-ray powder diffraction patterns of the starting clay (bentonite), TiO_2-pillared bentonite, and iron ion-exchanged TiO_2-pillared bentonites are shown in Fig. 1. XRD

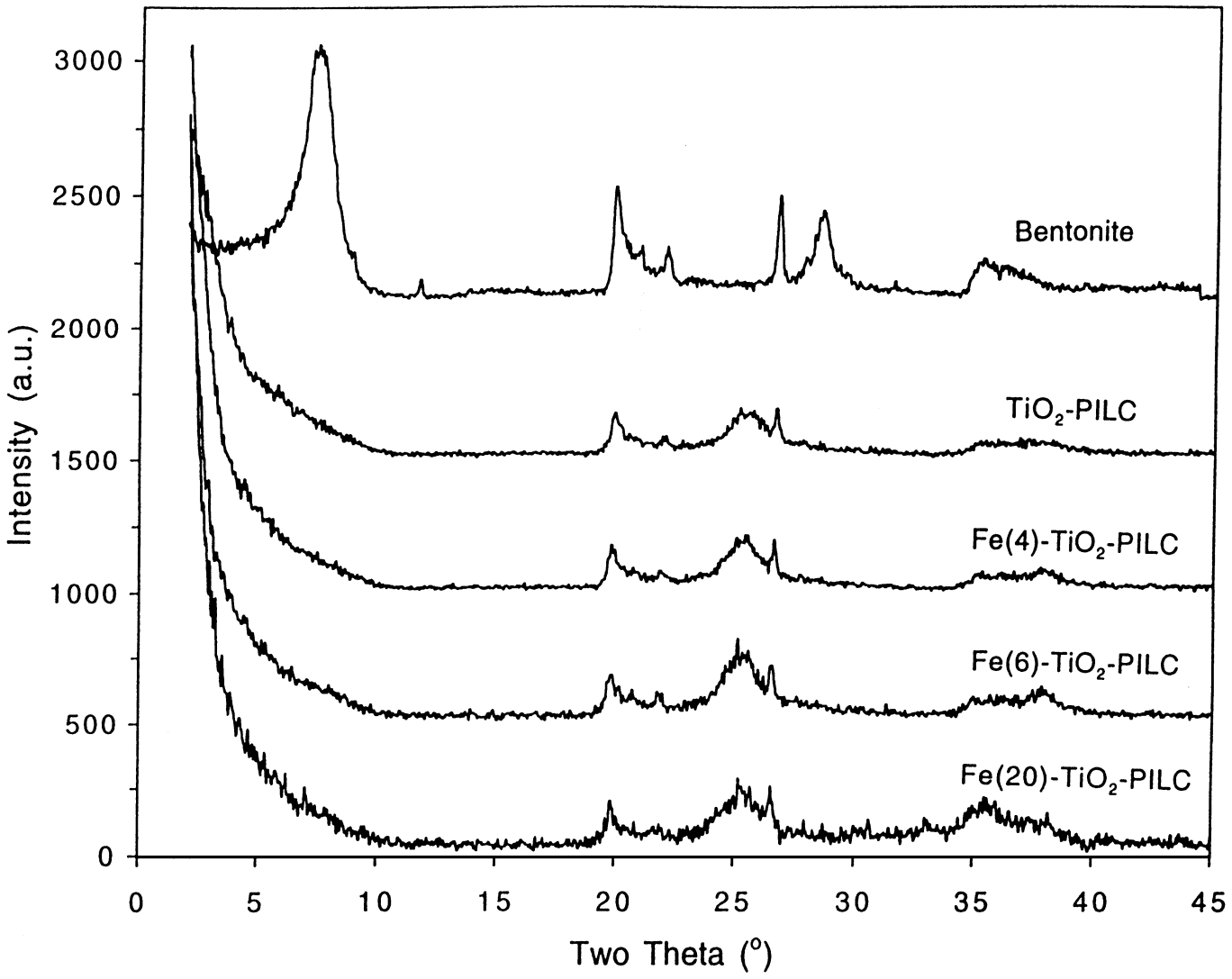

FIG. 1. XRD patterns of bentonite, TiO_2–PILC, and Fe–TiO_2–PILC catalysts.

patterns of smectite clays (e.g., bentonite) generally show basal 001 reflection and two-dimensional diffraction *hk* only, and other *hkl* diffractions are usually not observed (21). The d_{100} peak for the unpillared bentonite was at $2\theta = 7.7^\circ$. The diffraction at 19.7° ($d = 0.45$ nm) was the summation of *hk* indices of (02) and (11), and the diffraction at 35.0° ($d = 0.26$ nm) was the summation of *hk* indices of (13) and (20) (9, 21). The peak at 26.5° ($d = 0.34$ nm) was the diffraction of (101) from quartz impurity. Upon intercalation, the d_{100} peak disappeared and the intensities of the other peaks decreased. Pillared clays that exhibit no (001) reflection have been referred to as delaminated pillared clays in the literature (10, 22). The delaminated pillared clays usually show larger pore diameter than laminated pillared clays. This will increase the diffusion rates for SCR. The broad peak at $2\theta = 25.3^\circ$ was assigned to (101) diffraction of anatase TiO_2. The XRD patterns of the Fe–TiO_2–PILC samples were similar to those of TiO_2–PILC, and no peak for Fe_2O_3 was observed, even when the Fe content reached 20.1% in Fe(20)–TiO_2–PILC. This indicated that the Fe_2O_3 formed in hydrolysis of iron ions at 50°C and then calcination at high temperature was dispersed well on the surface of TiO_2–PILC.

Main Characteristics of Fe–TiO_2–PILC

The BET surface areas, pore volumes, and pore size distributions of the Fe–TiO_2–PILC catalysts are summarized in Table 2 and Fig. 2. The TiO_2–PILC showed a BET surface area of 310 m^2/g, which is much larger than that of unpillared bentonite (30 m^2/g). After iron ion-exchange and calcination at 400°C for 6 h, the surface areas of Fe–TiO_2–PILC decreased to 246–237 cm^2/g, as shown in Table 2. The pore volumes of all the samples were about 0.3 cm^3/g. Each of

TABLE 2

Characterization of the Catalysts

Sample	Surface area (m^2/g)	Pore volume (cm^3/g)	Bimodal pore diameters (nm)	H_2/Fe (TPR) (mol/mol)
TiO_2–PILC	310	0.32	2.2, 3.7	0.46
Fe(4)–TiO_2–PILC	246	0.29	2.3, 3.7	0.49
Fe(6)–TiO_2–PILC	245	0.31	2.4, 3.7	0.49
Fe(20)–TiO_2–PILC	237	0.33	2.7, 3.6	—

the samples showed a bimodal macropore size distribution. The TiO_2–PILC had distributions with two maxima at 2.2 and 3.7 nm (Fig. 2). After iron ions were exchanged with TiO_2–PILC, there was a decrease in the macropore volume at both the two peaks, but the macropore volume for the smaller pore decreased more sharply with the increase of iron content. In contrast, the pore volume of the bigger pore (>5 nm) increased with iron content.

The reducibility of the TiO_2–PILC and Fe–TiO_2–PILC catalysts was characterized by H_2-TPR analysis. As shown in Fig. 3, a weak reduction peak at 605°C appeared on the TiO_2–PILC sample, which is attributed to the reduction of iron because other species, e.g., TiO_2, SiO_2, Al_2O_3, MgO,

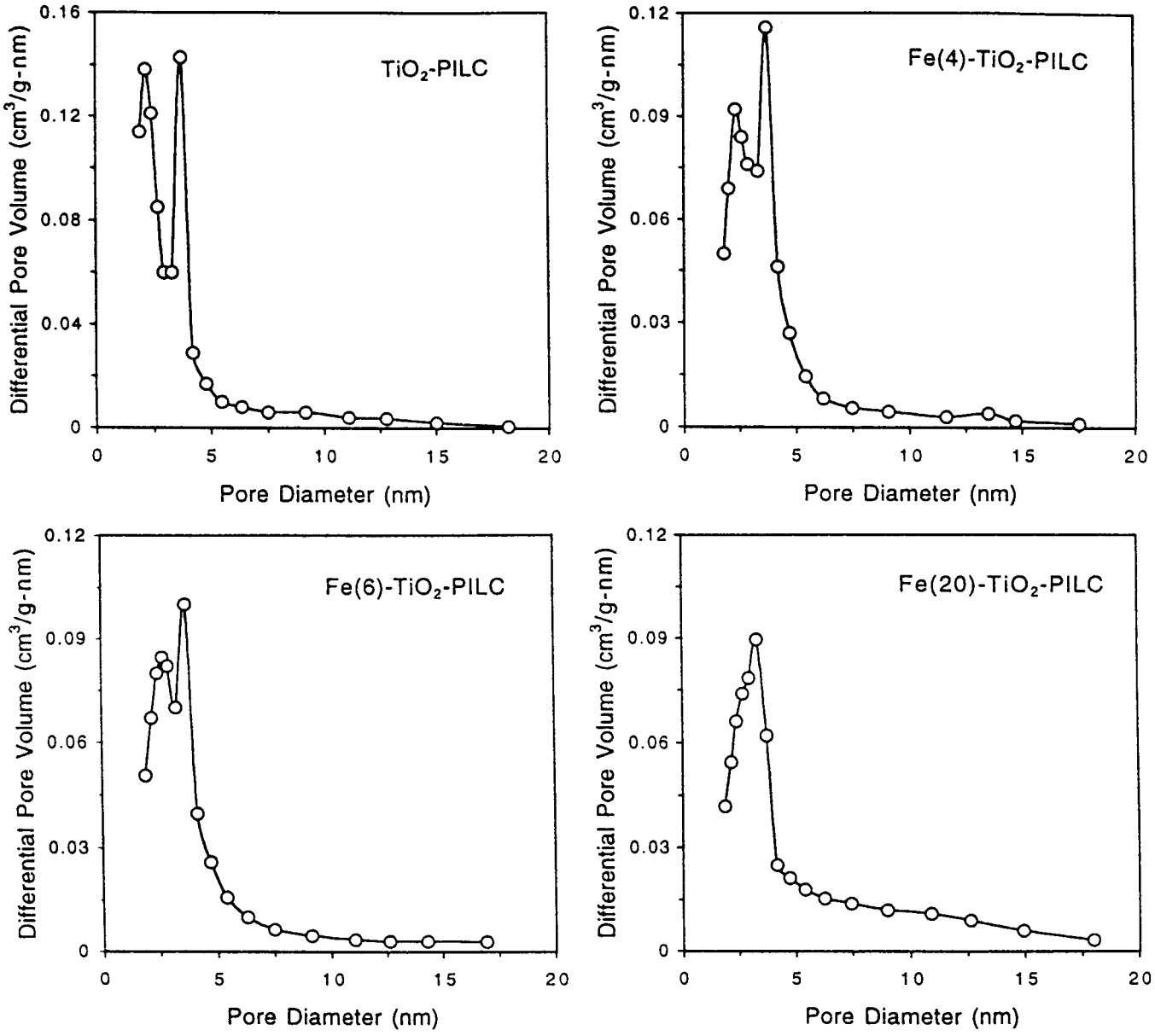

FIG. 2. Pore size distribution for TiO_2–PILC and Fe–TiO_2–PILC catalysts.

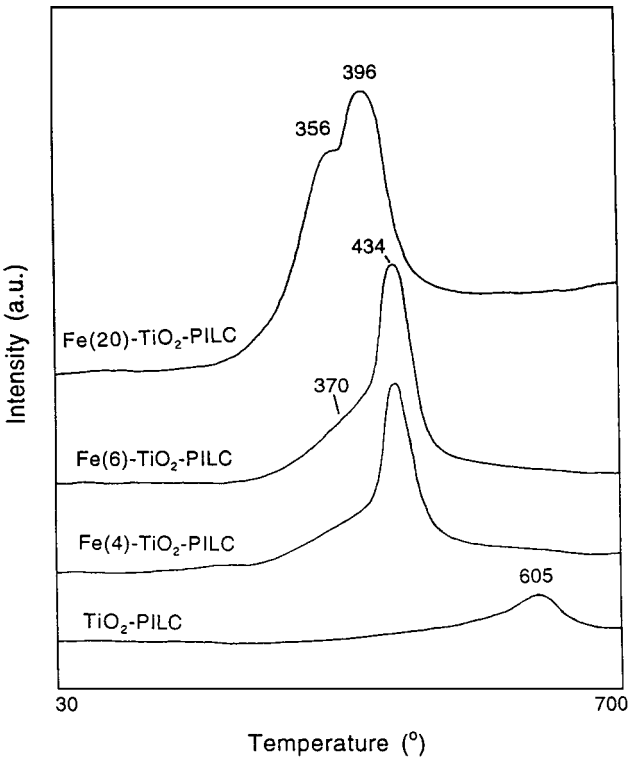

FIG. 3. H_2-TPR profiles of TiO_2–PILC and Fe–TiO_2–PILC catalysts.

CaO, and Na_2O, can not be reduced by H_2 under this condition. Fe(4)–TiO_2–PILC and Fe(6)–TiO_2–PILC showed one peak at 434°C and a shoulder at about 370°C, which can be assigned to the reduction of iron species at two different sites. The H_2 consumptions expressed as the ratio of H_2/Fe for the three samples are near 0.5 (Table 2), indicating that the Fe species are reduced from +3 to +2. Considering the facts that pure Fe_2O_3 will be reduced to metallic iron at about 530°C by H_2 in one step and the ratio H_2/Fe is 1.5 (23), we can reasonably deduce that iron in the three samples existed in the form of isolated Fe^{3+} ions. For Fe(20)–TiO_2–PILC, one peak at 396°C and a shoulder at 356°C were also detected, but the TPR profile did not return to the base line at 700°C (Fig. 3). The continuous consumption of H_2 suggests that the iron species in the Fe(20)–TiO_2–PILC sample was not reduced completely at 700°C.

SCR Catalytic Activity

The pure TiO_2–PILC showed little activity for NO_x reduction at 250–450°C. For instance, only 16.0% NO_x conversion was obtained at 400°C under the conditions of 1000 ppm NO, 1000 ppm NH_3, 2% O_2, and GHSV = 113 000 l/h. However, all of the Fe–TiO_2–PILC catalysts showed very high NO_x conversions under the same conditions, as shown in Table 3. For Fe(4)–TiO_2–PILC, the SCR activity increased with temperature at 300–450°C, while for other Fe–TiO_2–PILC catalysts with higher iron contents, the NO_x conversions increased with temperature at first, passing through a maximum at 375 or 400°C, then decreased slightly at higher temperatures. At lower temperatures (e.g., 300°C), the activity increased with iron content. The activities of the Fe–TiO_2–PILC catalysts were higher than that of the 4.4% V_2O_5–8.2% WO_3/TiO_2 catalyst at higher reaction temperatures (≥375°C). In addition, no or little N_2O was formed on the Fe–PILC catalysts in the SCR reaction. The product selectivities for N_2 on the Fe–TiO_2–PILC catalysts were significantly better than those of the 4.4% V_2O_5–8.2% WO_3/TiO_2 catalyst, especially at higher temperatures. The nitrogen balance was above 95% in this work.

The SCR activity can also be represented quantitatively by turnover frequency (TOF) and first-order rate constant (k) (since the reaction is known to be first order with respect to NO under stoichiometric NH_3 conditions on a variety of catalysts (1)). Assuming a plug flow reactor (in a fixed bed of catalyst) and freedom from diffusion limitation, the rate constant can be calculated from the NO_x conversion (X) by

$$k = -\frac{F_0}{[\mathrm{NO}]_0 W} \ln(1 - X), \qquad [1]$$

where F_0 is the molar NO feed rate, $[NO]_0$ is the molar NO concentration at the inlet (at the reaction temperature), and W is the catalyst amount (g). TOF is defined as the number of NO_x molecules converted per Fe per second. From the NO_x conversions and Fe contents or catalyst amounts in the above catalysts, TOF and first-order rate constants were calculated and compared in Table 3. Note that, because both V_2O_5/TiO_2 and WO_3/TiO_2 are active in the SCR reaction (1), we did not calculate the TOF of 4.4% V_2O_5–8.2% WO_3/TiO_2 catalyst. From Table 3, we can see that the TOF of the Fe–TiO_2–PILC catalysts decreased with the increase of Fe content. The k value of Fe(6)–TiO_2–PILC was 27% higher than that of the commercial vanadia catalyst at 400°C.

Effects of H_2O and SO_2

Because the resistance to H_2O and SO_2 is an important factor for the SCR reaction, we also studied the effects of H_2O and SO_2 on the catalytic performance of the Fe–TiO_2–PILC and 4.4% V_2O_5–8.2% WO_3/TiO_2 catalysts. After 8% H_2O and 1000 ppm SO_2 were added to the reactants, the NO_x conversions decreased at low temperatures (e.g., 300°C) on these catalysts (comparing Table 3 with Table 4). At temperatures above 350°C, the catalytic activities increased significantly on the Fe–TiO_2–PILC catalysts in the presence of H_2O and SO_2. The maximum NO_x conversion reached 95–98% on the Fe–TiO_2–PILC catalysts, which was more (8–10%) than that of the commercial V_2O_5–WO_3/TiO_2 catalyst. Judging from the values of the first-order rate constant k at 400°C, the Fe–TiO_2–PILC catalysts were about twice as active as the vanadium catalyst

TABLE 3

Catalytic Performance of Fe–TiO_2–PILC Catalysts in the Absence of H_2O and SO_2[a]

Catalyst	Temperature (°C)	NO_x conv. (%)	Selectivity (%)		TOF[b] × 10^3 (s^{-1})	k[c] (cm^3/g/s)
			N_2	N_2O		
Fe(4)–TiO_2–PILC	300	52.5	100	0	1.16	59.6
	350	78.5	100	0	1.74	134
	375	86.2	100	0	1.91	179
	400	90.0	100	0	1.99	217
	450	91.0	100	0	2.01	243
Fe(6)–TiO_2–PILC	300	57.0	100	0	0.920	67.6
	350	83.5	100	0	1.35	157
	375	90.2	100	0	1.45	210
	400	92.5	99.5	0.5	1.49	244
	450	89.0	99.4	0.6	1.44	223
Fe(8)–TiO_2–PILC	300	69.5	99.1	0.9	0.858	95.1
	350	86.0	98.7	1.3	1.06	171
	375	89.0	98.6	1.4	1.10	200
	400	89.0	98.4	1.6	1.10	208
	450	83.5	97.4	2.6	1.03	182
Fe(20)–TiO_2–PILC	300	75.3	98.9	1.1	0.358	112
	350	88.0	98.8	1.2	0.418	185
	375	89.0	98.6	1.4	0.423	200
	400	87.0	98.5	1.5	0.413	192
	450	80.0	97.2	2.8	0.380	163
Ce–Fe(5)–TiO_2–PILC[d]	300	45.0	100	0	1.57	95.8
	350	77.5	100	0	2.71	260
	375	89.5	100	0	3.13	408
	400	91.5	100	0	3.20	464
	450	90.0	99.4	0.6	3.15	465
4.4% V_2O_5–8.2% WO_3/TiO_2	300	82.0	98.6	1.4	—	137
	350	87.0	97.1	2.9	—	177
	375	88.0	95.2	4.8	—	192
	400	87.0	91.8	8.2	—	192
	450	68.0	81.3	18.7	—	115

[a] Reaction conditions: 0.2 g catalyst, [NO] = [NH_3] = 1000 ppm, [O_2] = 2%, He = balance, total flow rate = 500 ml/min, and GHSV = 113 000 l/h.

[b] TOF (turnover frequency) is defined as the number of NO_x molecules converted per Fe per second.

[c] First-order rate constant, as defined in the text, calculated by Eq. [1].

[d] 0.1 g catalyst was used.

under the same conditions with SO_2 and H_2O. The maximum k values of the Fe–TiO_2–PILC catalysts were also higher than those of Fe_2O_3/TiO_2, Fe_2O_3/Al_2O_3, Fe_2O_3/TiO_2–PILC, and $Fe_2O_3 + Cr_2O_3$/TiO_2–PILC catalysts (6, 7). Moreover, H_2O and SO_2 increased slightly the product selectivities to N_2 on the three catalysts, which may be attributed to a decrease of NH_3 oxidation by O_2. The improvement of catalytic activity by the presence of H_2O and SO_2 was attributed to the increase of surface acidity of the catalysts, as supported by FT–IR evidence shown in the next section. In fact, H_2O and SO_2 have different effects on the catalytic activity for the SCR reaction. In a separate experiment, H_2O alone decreased the activity of Fe–TiO_2–PILC at low temperatures, as shown in Fig. 4. As the reaction temperature was increased, the negative effect diminished. However, SO_2 had little effect on NO_x conversion at low temperatures for Fe–TiO_2–PILC, but it increased the NO_x conversion at high temperatures. Hence, the total effect of H_2O and SO_2 on the Fe–TiO_2–PILC catalysts for the SCR reaction showed a decrease in activity at low temperatures but an increase at high temperatures.

Effect of Ce Promoter

As seen in Tables 3 and 4, Ce–Fe(5)–TiO_2–PILC was very active in the SCR reaction. Although only 0.1 g catalyst (i.e., GHSV = 226 000 l/h) was used, very high NO conversions were still obtained. Judging from the TOF and k values, the activities for this catalyst were much higher than those of Fe–TiO_2–PILC catalysts both with and without H_2O and SO_2. This indicates that cerium is a good promoter for the Fe–TiO_2–PILC catalysts in the SCR reaction. Further study

TABLE 4

Catalytic Performance of Fe–TiO_2–PILC Catalysts in the Presence of H_2O and SO_2[a]

Catalyst	Temperature (°C)	NO_x conv. (%)	Selectivity (%)		TOF[b] $\times 10^3$ (s^{-1})	k[c] (cm^3/g/s)
			N_2	N_2O		
Fe(4)–TiO_2–PILC	300	39.5	100	0	0.873	40.3
	350	90.0	100	0	1.99	201
	375	96.0	100	0	2.12	292
	400	98.1	100	0	2.17	373
	450	97.1	100	0	2.15	358
Fe(6)–TiO_2–PILC	300	46.9	100	0	0.756	50.7
	350	92.4	100	0	1.49	224
	375	97.0	100	0	1.56	318
	400	98.0	99.4	0.6	1.58	368
	450	96.2	99.2	0.8	1.55	331
Fe(8)–TiO_2–PILC	300	52.5	99.5	0.5	0.648	59.6
	350	91.0	99.3	0.7	1.12	210
	375	94.0	99.0	1.0	1.16	255
	400	95.0	98.8	1.2	1.17	282
	450	90.0	98.5	1.5	1.11	233
Fe(20)–TiO_2–PILC	300	66.6	99.2	0.8	0.361	87.8
	350	91.8	99.1	0.9	0.436	218
	375	94.0	98.9	1.1	0.447	255
	400	95.5	98.5	1.5	0.454	292
	450	90.5	97.8	2.2	0.430	238
Ce–Fe(5)–TiO_2–PILC[d]	300	37.0	100	0	1.30	74.0
	350	85.5	100	0	2.99	336
	375	94.0	100	0	3.29	510
	400	96.0	100	0	3.36	606
	450	95.0	99.5	0.5	3.33	606
4.4%V_2O_5–8.2%WO_3/TiO_2	300	76.0	98.9	1.1	—	114
	350	87.0	98.1	1.9	—	177
	375	88.0	96.9	3.1	—	192
	400	87.0	94.8	5.2	—	192
	450	72.0	90.2	9.8	—	129

[a] Reaction conditions: 0.2 g catalyst, [NO] = [NH_3] = 1000 ppm, [O_2] = 2%, [H_2O] = 8%, [SO_2] = 1000 ppm, He = balance, total flow rate = 500 ml/min, and GHSV = 113 000 l/h.
[b] Defined in Table 3.
[c] Defined in Table 3.
[d] 0.1 g catalyst was used.

on the promoting role of cerium is in progress. The maximum activity of Ce–Fe(5)–TiO_2–PILC was more than three times that of the commercial V_2O_5–WO_3/TiO_2 catalyst in the presence of H_2O and SO_2.

Effect of O_2

Previous studies of SCR catalysts have shown the importance of oxygen in the reaction (1). The effect of oxygen on catalytic activity was also studied in this work. As shown in Fig. 5, Fe–TiO_2–PILC showed low activity for the reduction of NO by NH_3 at 300–400°C in the absence of oxygen. However, when a little O_2 was introduced to the reactants, NO_x conversion increased sharply. When O_2 concentration was more than 0.5%, NO_x conversion showed no further change. This indicated that O_2 played a significant promoting role in the SCR reaction. The importance of O_2 was also verified by another experiment. After O_2 was shut off from the reactants at 375°C, the NO_x conversion declined sharply (Fig. 6). This is similar to the behavior on iron oxide doped catalysts (1, 5), but different from supported vanadia catalysts (1). On vanadia catalysts, NO conversion declined steadily over a period of time after O_2 was turned off. The different transient behaviors to O_2 indicated a different reaction mechanism for the Fe–TiO_2–PILC catalyst. The lattice oxygen may not be involved in the SCR reaction (as in the case for the vanadia catalyst) while the adsorbed oxygen species on the surface may play an important role for the pillared clay catalyst.

SO_2 Oxidation Activity

Oxidation of SO_2 to SO_3 causes severe problems for the SCR reaction due to the formation of sulfuric acid,

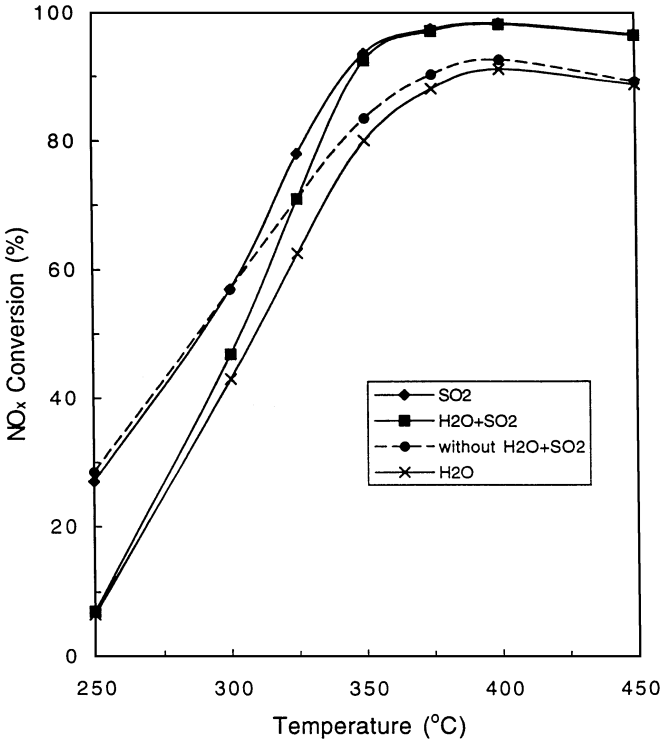

FIG. 4. Effect of H_2O and SO_2 on the catalytic activity for Fe(6)–TiO_2–PILC catalyst. Reaction conditions: 0.2 g catalyst, [NO] = [NH_3] = 1000 ppm, [O_2] = 2%, [H_2O] = 8%, [SO_2] = 1000 ppm, He = balance, total flow rate = 500 ml/min, and GHSV = 113 000 l/h.

ammonium sulfate, and other compounds, which result in corrosion and plugging of the reactor and heat-exchangers (1). Vanadia-based catalysts have a high SO_2 oxidation activity, which has been a major concern in SCR operations. Efforts have been made either to add certain oxides (such as WO_3 or GeO_2) to V_2O_5 catalyst or to use non-V_2O_5 catalysts for the purpose of decreasing SO_2 oxidation activity while maintaining high NO_x reduction activity (1). Using the wet chemical method described in the foregoing to quantitatively measure the amounts of SO_3 generated in the reaction effluents, the conversions for SO_2 to SO_3 were 1.0, 1.2, 2.1, and 8.0%, respectively, for the Fe(4)–TiO_2–PILC, Fe(6)–TiO_2–PILC, Fe(20)–TiO_2–PILC, and 4.4% V_2O_5–8.2% WO_3/TiO_2 catalysts. The catalysts containing iron yield much lower SO_3 (by 74–88%) than the V_2O_5-based catalyst. Results by Clark *et al.* (24), in their study of alumina-supported iron oxide and vanadium oxide catalysts, also showed that Fe_2O_3 was less active in SO_2 oxidation than V_2O_5.

Surface Acidity of the Catalysts

The surface acidity and the strength of acid can be determined by using ammonia as a probe molecule. Such information was obtained by studying the FTIR spectra of the adsorbed NH_3. The spectra of adsorbed ammonia at room temperature on the samples pretreated at 450°C in He for 30 min are shown in Fig. 7. A strong band at 1451 cm^{-1} and three weaker bands at 1670, 1596, and 1242 cm^{-1} were detected on the TiO_2–PILC sample (Fig. 7). The bands at 1670 and 1451 cm^{-1} were due to the symmetric and asymmetric bending vibrations of NH_4^+ that was chemisorbed on the Brønsted acid sites, while the bands at 1596 and 1242 cm^{-1} could be assigned to asymmetric and symmetric vibrations of the N–H bonds in NH_3 coordinately linked to Lewis acid sites (25–27). When iron ions were exchanged to TiO_2–PILC, the intensities of the ammonia absorption bands were found to decrease slightly. For all the samples, there were more Brønsted acid sites than Lewis acid sites at room temperature. With an increase in temperature, the intensities of the above bands decreased, as shown in Fig. 8, indicating desorption of NH_3. Upon heating to 350°C, no NH_4^+ or coordinated NH_3 were detected on the surface of the Fe(6)–TiO_2–PILC catalyst.

The fresh Fe(6)–TiO_2–PILC was treated at 400°C in a flow of 5% H_2O/He for 15 min and then cooled to room temperature in H_2O/He. A strong band centering at 1630 cm^{-1} appeared (not shown), which can be attributed to O–H bending vibration of adsorbed water. After the sample adsorbed NH_3 for 30 min at room temperature, the band due to adsorbed H_2O became weaker, while a strong band at 1461 cm^{-1} and three weaker bands at 1687, 1597, and

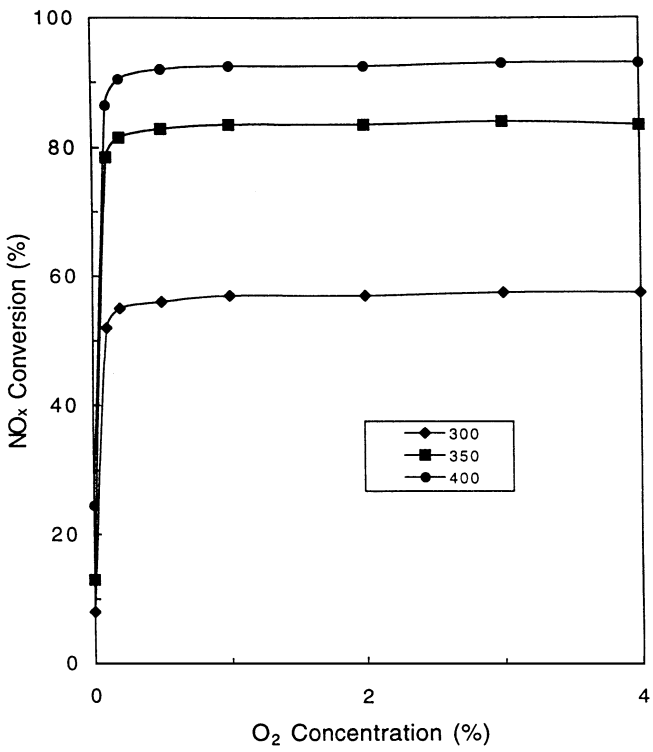

FIG. 5. Effect of O_2 concentration on the catalytic activity for Fe(6)–TiO_2–PILC catalyst at different temperatures. Reaction conditions: 0.2 g catalyst, [NO] = [NH_3] = 1000 ppm, [O_2] = 0–4%, He = balance, total flow rate = 500 ml/min, and GHSV = 113 000 l/h.

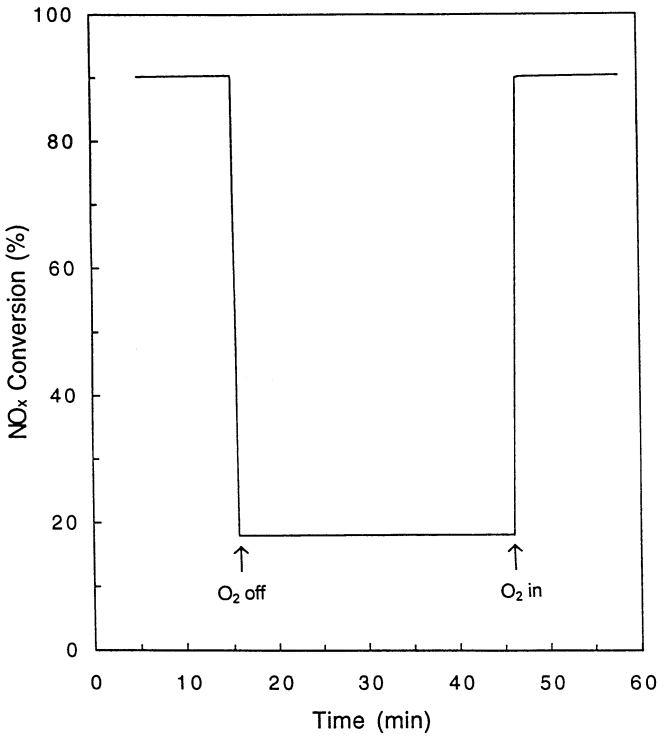

FIG. 6. Transient response on Fe(6)–TiO_2–PILC upon switching off and on O_2 at 375°C. Reaction conditions: 0.2 g catalyst, [NO] = [NH_3] = 1000 ppm, [O_2] = 2% (when used), He = balance, total flow rate = 500 ml/min, and GHSV = 113 000 l/h.

1231 cm^{-1} appeared (Fig. 8). This suggested that ammonia displaced some of the adsorbed water to form coordinated NH_3 and/or consumed some of the surface hydroxyl groups to form NH_4^+. As compared with the He-pretreated Fe(6)–TiO_2–PILC, the NH_4^+ band at 1461 cm^{-1} on the H_2O-pretreated sample was slightly stronger (Fig. 8). This result suggests that H_2O did not inhibit the adsorption of ammonia on the Fe–TiO_2–PILC surface under SCR reaction conditions.

After Fe(6)–TiO_2–PILC was treated at 400°C for 15 min in a flow of $SO_2/H_2O/O_2$ (1000 ppm SO_2, 2% O_2, 5% H_2O, and He as balance) followed by purging for 10 min by He, a strong peak at 1364 cm^{-1} and two shoulders at 1303 and 1237 cm^{-1} appeared, which suggested that surface sulfate species were formed on the Fe–TiO_2–PILC catalyst (as shown in Fig. 9). The 1364 and 1237 cm^{-1} bands were assigned to asymmetric and symmetric S=O stretching frequencies of an "organic" sulfate species which has covalent S=O double bonds. The characteristics of the "organic" sulfate species are the remarkably high S=O stretching frequencies (asymmetric at 1440–1350 cm^{-1} and symmetric at about 1230 cm^{-1}) (28, 29). The band at 1303 cm^{-1} was attributed to a chelating bidentate inorganic SO_4^{2-} bond to iron which has only ionic SO bonds with a partial double bond character. When the temperature was decreased, the intensities of the "organic" sulfate bands (1364 and 1237 cm^{-1}) decreased, while the band (1303 cm^{-1}) of inorganic sulfate species became stronger and shifted gradually to lower wavenumbers (Fig. 9). This suggested a structural transformation from "organic" sulfate to inorganic sulfate due to interactions with residual water (28). At room temperature, the chelating bidentate inorganic sulfate became the dominating sulfate species and a peak at 1632 cm^{-1} due to adsorbed H_2O appeared on the sample. Similar results were also obtained on the other Fe–TiO_2–PILC catalysts. In contrast, only a weak peak at 1357 cm^{-1} was detected on TiO_2–PILC after it was treated in a flow of $SO_2 + O_2 + H_2O$/He mixture at 400°C for 15 min (Fig. 9), indicating TiO_2–PILC alone does not form a significant amount of sulfate at 400°C. When the sample was cooled to room temperature, two weak peaks at 1628 cm^{-1} (due to adsorbed H_2O) and 1347 cm^{-1} (due to sulfate species) were detected on the TiO_2–PILC sample (Fig. 9).

As shown in Fig. 10, after the Fe–TiO_2–PILC samples (that were pretreated by $SO_2 + O_2 + H_2O$/He) adsorbed NH_3 for 30 min at room temperature followed by purging with He for 15 min, the sulfate band at 1266 cm^{-1} shifted to 1236 cm^{-1}. At the same time, a very strong band at 1453 cm^{-1} and two weaker bands at 1670 and 1598 cm^{-1} appeared. This indicates that the surface sulfate species

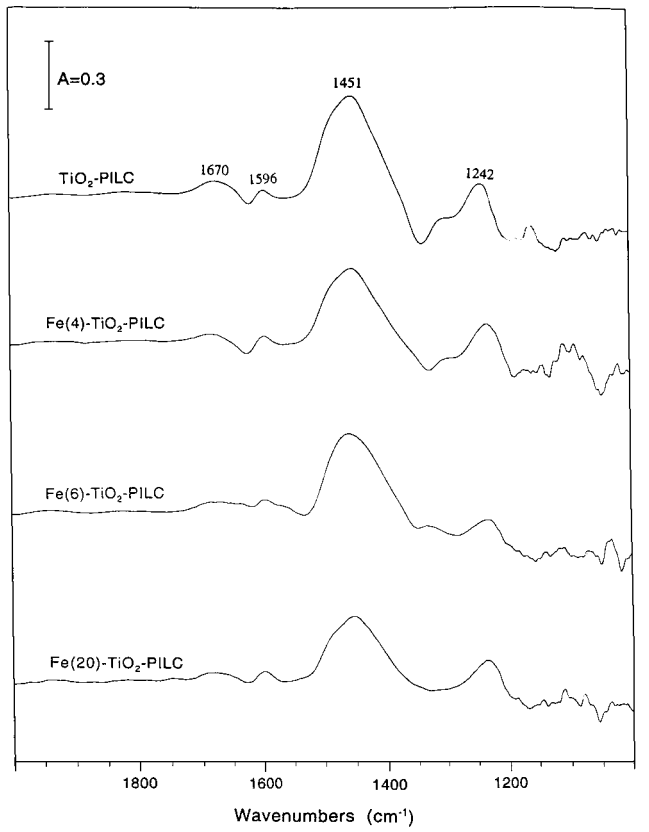

FIG. 7. FT-IR spectra of chemisorbed NH_3 at 25°C on TiO_2–PILC and Fe–TiO_2–PILC catalysts.

increased the Brønsted acidity of the three Fe–TiO_2–PILC samples significantly. The transfer of the electrons from the adsorbed ammonia to the sulfate species resulted in a decrease in the S–O vibration frequencies. The band at 1242 cm^{-1} due to symmetric vibration of the NH_3 coordinated to Lewis acid sites was overlapped by the sulfate band at 1236 cm^{-1}. The Brønsted acidity of the TiO_2–PILC pretreated by $SO_2 + O_2 + H_2O$/He only showed a slight increase as compared to the fresh TiO_2–PILC, as shown in Fig. 10. This is consistent with the above result that little sulfate species formed on this sample after it was treated by $SO_2 + O_2 + H_2O$/He at 400°C.

When the NH_3-adsorbed Fe(6)–TiO_2–PILC (that was pretreated by $SO_2 + O_2 + H_2O$/He at 400°C) was heated in a flow of He, the ammonia began to desorb from the sample surface and resulted in a gradual decrease in the intensity of NH_4^+ (Fig. 11). At the same time, the band at 1234 cm^{-1} became broader and shifted to higher wavenumbers. This suggested that a transformation occurred from inorganic sulfate to "organic" sulfate due to the removal of molecular water. At 350°C, one can still see clearly NH_4^+ on the Fe(6)–TiO_2–PILC surface (Fig. 11). This indicates that the surface sulfate species also enhanced the acid strength of the Fe–TiO_2–PILC because no NH_4^+ ions were detected on the fresh sample at this temperature (Fig. 8). At 400°C, only sulfate species were detected on the Fe–TiO_2–PILC surface.

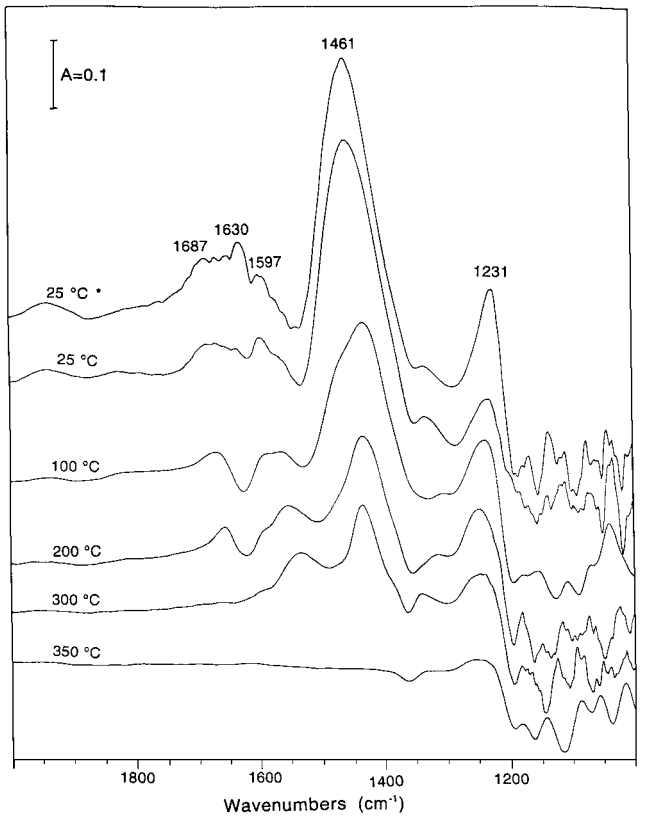

FIG. 8. FT-IR spectra of chemisorbed NH_3 on Fe(6)–TiO_2–PILC at different temperatures. Asterisk indicates sample pretreated by H_2O/He.

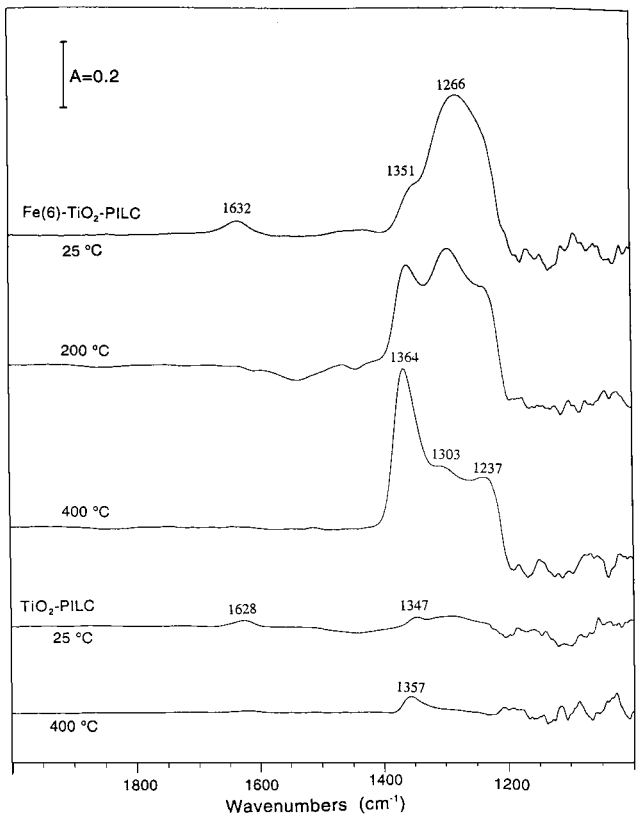

FIG. 9. FT-IR spectra at different temperatures of Fe(6)–TiO_2–PILC and TiO_2–PILC pretreated by $SO_2 + O_2 + H_2O$/He at 400°C.

DISCUSSION

Catalytic Performance for NO_x Reduction and Characteristics of Fe–TiO_2–PILC

TiO_2–PILC was studied as SCR catalyst by ammonia in our previous study (15), but it showed only moderate activities for NO_x reduction between 200 and 450°C. When iron oxide was doped (7, 14) or iron ions were exchanged with TiO_2–PILC(14), the activities for NO_x reduction increased markedly. It is evident that iron oxide and iron ions on the TiO_2–PILC played an important role in this reaction. At lower temperatures (e.g., 300°C), NO_x conversion increased with increasing iron content in the Fe–TiO_2–PILC catalysts. However, at higher temperatures, NO_x conversions were lower on the catalysts with higher iron contents (Tables 3 and 4). For all the catalysts, water vapor decreased their activities, while SO_2 or $SO_2 + H_2O$ improved the catalytic activities at high temperatures (Fig. 4 and Table 4). The Fe–TiO_2–PILC catalysts showed about twice the activity as compared to the commercial V_2O_5–WO_3/TiO_2 catalyst in

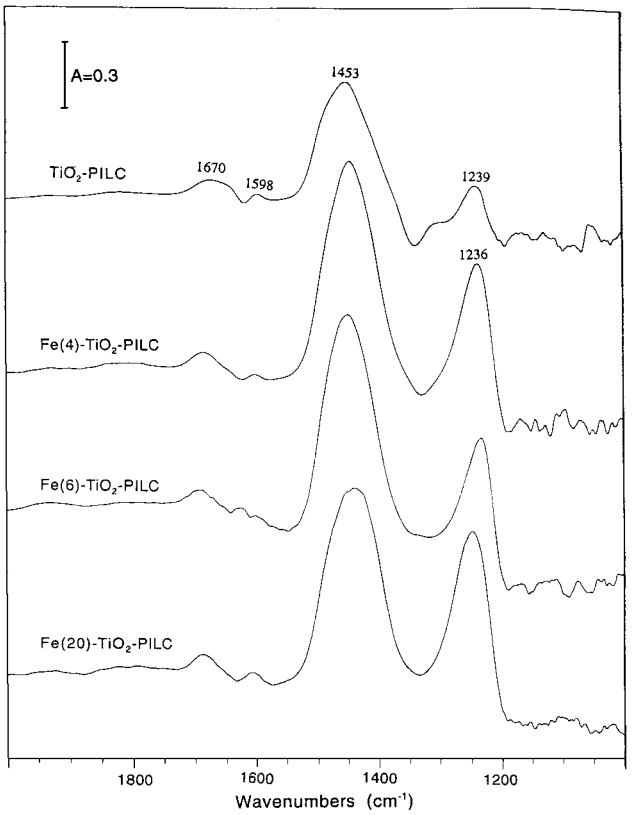

FIG. 10. FT-IR spectra of chemisorbed NH_3 at 25°C on TiO_2–PILC and Fe–TiO_2–PILC catalysts pretreated by $SO_2 + O_2 + H_2O$/He at 400°C.

the presence of H_2O and SO_2. Moreover, the Ce-promoted Fe–TiO_2–PILC showed more than three times the activity of the commercial catalyst. (The role of Ce will be addressed in a separate study.) The product selectivities for N_2 on the Fe–TiO_2–PILC catalysts were also higher than that for the commercial catalyst, especially at high temperatures (Tables 3 and 4). The latter yielded much more N_2O at high temperatures (e.g., 450°C). In the SCR reaction, N_2O results from oxidation of NH_3 by O_2 and/or partial reduction of NO_x by NH_3 (1). Vanadia catalysts are very active in the oxidation of ammonia to form N_2, N_2O, and NO, and hence result in a sharp decrease in NO_x conversion due to the consumption of ammonia by O_2 at 450°C. By comparison, the Fe–TiO_2–PILC catalysts showed low N_2O selectivities and high NO_x conversions at high temperatures (e.g., 450°C), which suggests that they had lower activities for ammonia oxidation. It has been reported that Fe_2O_3 was less active in the oxidation of ammonia than V_2O_5 (30). Compared to the commercial catalyst, the activities for SO_2 oxidation (to SO_3) of the Fe–TiO_2–PILC catalysts were also significantly lower (by 74–88%).

In this work, the ion exchange process was performed under the condition of pH 1.5. The $Fe(NO_3)_3$ solution contains about 75% Fe^{3+} and 25% $Fe_2(OH)_2^{4+}$ ions at room temperature (31). They can exchange with cations in TiO_2–PILC, i.e., mainly H^+, and also Na^+, K^+, and Mg^{2+}. After the Fe-exchanged TiO_2–PILC samples were calcined at 400°C, some $Fe_2(OH)_2^{4+}$ was decomposed to Fe_2O_3 and Fe^{3+} via

$$2\ Fe_2(OH)_2^{4+} \rightarrow Fe_2O_3 + 2\ Fe^{3+} + H_2O + 2\ H^+. \quad [2]$$

Hence, the iron in the Fe(4)–TiO_2–PILC and Fe(6)–TiO_2–PILC catalysts with lower iron contents existed mainly in the form of isolated Fe^{3+} ions, as shown by the TPR results (Fig. 3). Ion exchange with pillared clay has been widely studied. Kukkadapu and Kevan (32) studied the cupric-ion-exchanged Al_2O_3-pillared laponite by using electron spin resonance (ESR) and electron spin echo modulation (ESEM) methods, and found that Cu^{2+} was directly anchored to alumina pillars. In the V-doped titania-pillared clay, Bahranowski *et al.* (33) also reported that the V dopant was bound to the titania pillars, from ESR results. From these results, it is reasonable to suggest that the Fe^{3+} ions were also probably bound to titania pillars in the Fe–TiO_2–PILC catalysts. For Fe(8)–TiO_2–PILC and Fe(20)–TiO_2–PILC catalysts, the ion exchange process was carried out at 50°C. Under that condition, some iron ions would be hydrolyzed to iron hydroxide and precipitated on the surface of TiO_2–PILC. This led to higher iron contents on the two samples. The iron oxide would block some of the smaller

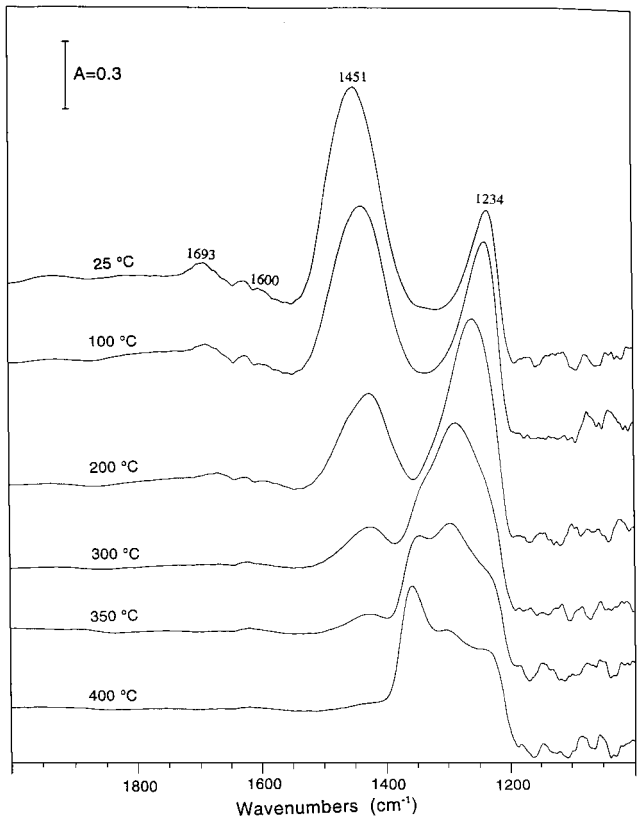

FIG. 11. FT-IR spectra at different temperatures of chemisorbed NH_3 on Fe(6)–TiO_2–PILC pretreated by $SO_2 + O_2 + H_2O$/He at 400°C.

pores in the TiO_2–PILC samples, as evidenced by the pore size distribution data (Fig. 2). When the iron content was increased to a high value, e.g., 20.1% in the Fe(20)–TiO_2–PILC sample, iron oxide would aggregate and form some big pores by themselves, as shown in Fig. 2. From the results above, the activities (i.e., NO_x conversion, TOF, and k) on Fe(4)–TiO_2–PILC and Fe(6)–TiO_2–PILC were higher than those on Fe(20)–TiO_2–PILC and Fe_2O_3-doped TiO_2–PILC (7). This suggests that iron ions were more active than iron oxide in the TiO_2–PILC.

Relationship between Catalytic Activity and Surface Acidity

It has been accepted that, in the SCR reaction, ammonia is adsorbed on the Brønsted or Lewis acid sites to form NH_4^+ or coordinated NH_3, then gaseous or adsorbed nitric oxides react with NH_4^+ or coordinated NH_3 to form N_2 and H_2O, although some different mechanisms were proposed (1, 13, 35–40). Hence the surface acidity of the catalyst is very important for the SCR reaction of NO_x by NH_3 (6, 7, 11–13). We now focus on its effect on the catalytic activity for NO_x reduction. As shown in Fig. 7, both Brønsted acid sites and Lewis acid sites exist in the TiO_2–PILC, with a larger proportion being Brønsted acid sites at room temperature. Pillars are the major sources for Lewis acidity on pillared clays (9). It is well known that Lewis acid sites exist on TiO_2 (13, 25, 41). Two sources for Brønsted acidity in pillared clays have been discussed in the literature. One derives from the structural hydroxyl groups in the clay layer (42). The most likely proton site for some smectites (e.g., montmorillonite) is located at the Al(VI)–O–MgO linkage, where Al(VI) is the octahedrally coordinated Al, and the Mg is one that has substituted an Al in the octahedral layer. Another source of proton derives from the cationic oligomers which upon heating decompose into metal oxide pillars and liberate protons. It has been reported that both Lewis and Brønsted acidities decrease with temperature of calcination (10, 42). The disappearance of Brønsted acidity is attributed to the migration of protons from the interlayer surfaces to the octahedral layer within the clay layer where they neutralize the negative charges at the substitution atoms (such as Mg). However, it is known that upon exposure to NH_3 the migration is reversed so the proton is again on the surface to form ammonium ions. When iron ions were exchanged with TiO_2–PILC, the Brønsted acidity decreased slightly. This suggests that some H^+ in the pillared clay were substituted by iron ions. With an increase in iron content, Brønsted acidity decreased (Figs. 7 and 10). This is in agreement with the decrease in TOF with increasing iron content (Tables 3, and 4). On the Fe–TiO_2–PILC catalysts, there was also a larger proportion of Brønsted acid sites than Lewis acid sites at room temperature. This is different from Fe_2O_3 and other Fe_2O_3-doped catalysts, e.g., Fe_2O_3/MgO, where only Lewis acid sites exist on the surface (4, 5, 35). Recently, Ito *et al.* (43) studied Ce-exchanged mordenite SCR catalyst by *in situ* IR. They observed that the NH_3 coordinated to the Lewis acid sites reacted with NO^+ at 100°C, but NH_4^+ ions bonded to Brønsted acid sites were stable; they did not react with nitrito species (NO_2^-) until the temperature was increased to above 300°C. This suggests that coordinated NH_3 is more easily oxidized by nitrogen oxide species than NH_4^+ ions. This may be used to explain the result that Fe–TiO_2–PILC showed much higher activities at high temperatures than Fe_2O_3 and Fe_2O_3-doped catalysts, because coordinated NH_3 is also more easily oxidized by oxygen than NH_4^+.

The H_2O molecules could adsorb on the surface of Fe–TiO_2–PILC. But after introducing ammonia, the adsorbed H_2O molecules were gradually displaced by ammonia. This is attributed to the fact that ammonia has a stronger basicity than H_2O. This suggests that water vapor will not inhibit the adsorption of ammonia on the Fe–TiO_2–PILC surface under the SCR reaction conditions. The decrease in NO_x conversion at lower temperatures in the presence of H_2O or $SO_2 + H_2O$ may be attributed to its inhibition to the desorption of the product H_2O from the surface, which is similar to the phenomenon on V_2O_5/TiO_2 catalyst (44).

When Fe–TiO_2–PILC catalysts were treated at 400°C in a flow of $SO_2 + O_2 + H_2O$/He, their Brønsted acidities and acid strengths increased significantly (Figs. 7, 8, 10, and 11). It is known that, when some metal oxides, such as Fe_2O_3, TiO_2, and ZrO_2, are treated by H_2SO_4 or $(NH_4)_2SO_4$ followed by calcination at high temperatures, or are treated by SO_2/O_2 at high temperatures, they will show very strong acidities and are thus referred to as superacid (29). XPS and IR measurements showed that sulfate species formed on the sample surface (29). When Fe–TiO_2–PILC was treated at 400°C in a flow of $SO_2 + O_2 + H_2O$/He mixture, SO_2 was oxidized to SO_3 by O_2 on the surface and a sulfate species was formed. These were identified in the above SO_2 oxidation and IR experiments (Fig. 9). The formation of surface sulfate increased the surface acidity of the Fe–TiO_2–PILC catalysts. Consequently, the adsorption amount of ammonia increased and also the adsorbed NH_4^+ ions were hard to desorb from the surface. Because TiO_2–PILC pretreated by $SO_2 + O_2 + H_2O$/He showed little increase in the surface acidity (Figs. 7 and 10), the increase of surface acidity on the Fe–TiO_2–PILC by the SO_2 treatment was attributed to the increase of acidity sites on iron ions or iron oxide. This also indicates that iron ions and iron oxide were more easily sulfated by SO_2/O_2 than TiO_2 in the Fe–TiO_2–PILC samples. The sulfate ions on iron oxide showed a characteristic IR absorption band at near 1375 cm^{-1} (28). In the case of sulfate ions, S=O has a covalent double bond and has a much stronger affinity to electrons as compared with that of a simple metal sulfate; hence, the Lewis acid strength of metal ions becomes substantially stronger by the inductive

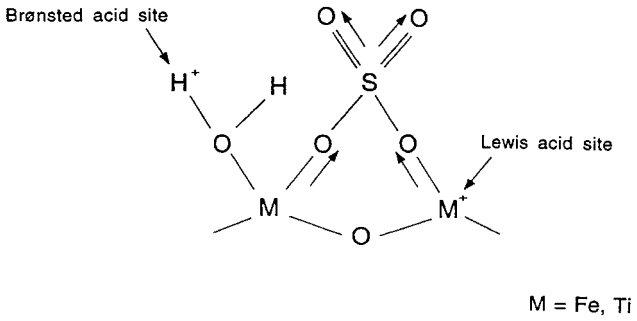

FIG. 12. Model for Brønsted acid sites and Lewis acid sites on sulfated iron oxide and titanium dioxide.

effect of S=O in the complex. A model for the acid sites is shown in Fig. 12. When a water molecule is bonded to the Lewis acid site, the Lewis acid site becomes a Brønsted acid site. This will increase the surface acidity of the catalysts containing iron and titania. The increase in the surface acidity will give rise to an increase in the catalytic activity. At low temperatures, SO_2 cannot be oxidized to SO_3 and thus sulfate ions cannot be formed. In this case, acidity cannot be increased. The decrease in activity for NO_x reduction at low temperatures by the presence of H_2O and SO_2 is mainly due to the inhibition of H_2O. In another experiment, when Fe(6)–TiO_2–PILC was pretreated by $SO_2 + O_2 + H_2O$/He for 30 min at 400°C, and then decreased to room temperature in He and subsequently used for the SCR reaction, it was found that the pretreated catalyst showed higher NO_x conversions than the fresh catalyst, e.g., 74.0% vs 57.0% at 300°C, 97.0% vs 83.5% at 350°C, and 98.0% vs 90.2% at 375°C. This result also indicates the promoting role of surface sulfate species and the importance of surface acidity for SCR reaction on the Fe–TiO_2–PILC catalysts.

CONCLUSIONS

The iron ion-exchanged TiO_2–PILC catalysts showed very high activities in the reduction of NO_x by NH_3 in the presence of excess oxygen. H_2O and SO_2 further increased the activity at high temperatures (i.e., above 300°C). A similar enhancement effect by H_2O and SO_2 was also observed for the Fe–ZSM-5 catalyst (45, 46). The Fe–TiO_2–PILC catalysts were about twice as active as the commercial V_2O_5–WO_3/TiO_2 catalyst in the presence of H_2O and SO_2. With Ce promoter, the activity was over three times that of the commercial catalyst. Moreover, as compared to V_2O_5–WO_3/TiO_2, the catalyst had higher N_2/N_2O product selectivities (e.g., 0–1% vs 9% N_2O at 400°C) and substantially lower activities (by 74–88%) for SO_2 oxidation to SO_3 under the same reaction conditions. The high activity and low N_2O selectivity on the Fe–TiO_2–PILC catalysts were attributed to their low activity in the oxidation of ammonia, as compared with vanadia catalysts. XRD measurements showed the same patterns for Fe–TiO_2–PILC and TiO_2–PILC, and no additional peaks due to iron oxide were detected on Fe–TiO_2–PILC. The activities of the Fe–TiO_2–PILC were well consistent with their surface acidities. The improvement in activities by $H_2O + SO_2$ was attributed to the increase of the surface acidity resulting from the formation of surface sulfate species of iron.

ACKNOWLEDGMENT

This work was supported by Electric Power Research Institute.

REFERENCES

1. Bosch, H., and Janssen, F., *Catal. Today* **2**, 369 (1988).
2. Okazaki, S., Kuroha, H., and Okuyama, T., *Chem. Lett.*, 45 (1985).
3. Tanabe, K., *Chem. tech.*, 628 (1991).
4. Bauerle, G. L., Wu, S. C., and Nobe, K., *Ind. Eng. Chem. Prod. Res. Dev.* **17**, 123 (1978).
5. Wong, W. C., and Nobe, K., *Ind. Eng. Chem. Prod. Res. Dev.* **25**, 179 (1986).
6. Chen, J. P., Hausladen, M. C., and Yang, R. T., *J. Catal.* **151**, 135 (1995).
7. Cheng, L. S., Yang, R. T., and Chen, N., *J. Catal.* **164**, 70 (1996).
8. Pinnavaia, T. J., *Science* **220**, 365 (1983).
9. Burch, R., *Catal. Today* **2**, 185 (1988).
10. Figueras, F., *Catal. Rev. Sci. Eng.* **30**, 457 (1988).
11. Okazaki, S., Kumasaka, M., Yoshida, J., Kosaka, K., and Tanabe, K., *Ind. Eng. Chem. Prod. Res. Dev.* **20**, 301 (1981).
12. Chen, J. P., and Yang, R. T., *J. Catal.* **125**, 411 (1990).
13. Topsøe, N. Y., Dumesic, J. A., and Topsøe, H., *J. Catal.* **151**, 241 (1995).
14. Yang, R. T., and Cichanowicz, J. E., "Pillared Clays as Catalysts for Selective Catalytic Reduction of NO," U.S. Patent 5,415,850, 1995.
15. Yang, R. T., Chen, J. P., Kikkinides, E. S., Cheng, L. S., and Cichanowicz, J. E., *Ind. Eng. Chem. Res.* **31**, 1440 (1992).
16. Bernier, A., Admaiai, L. F., and Grange, P., *Appl. Catal.* **77**, 269 (1991).
17. Kato, A., Matsuda, S., Nakajima, F., Imanari, M., and Watanabe, Y., *J. Phys. Chem.* **85**, 1710 (1981).
18. Sterte, J., *Clays Clay Miner.* **34**, 658 (1986).
19. Tuenter, G., Leeuwen, W. F. V., and Snepvangers, L. J. M., *Ind. Eng. Chem. Prod. Res. Dev.* **25**, 633 (1986).
20. Tanev, P. T., and Vlaev, L. T., *J. Colloid Interface Sci.* **160**, 110 (1993).
21. Bailey, S. W., *in* "Structures of Clay Minerals and Their X-Ray Indentification" (G. W. Brindley and G. Brown, Eds.), Mineralogical Society Monograph, Vol. 5. Mineralogical Society, London, 1980.
22. Pinnavaia, T. J., Tzou, M. S., Landau, S. D., and Raythatha, R., *J. Mol. Catal.* **27**, 195 (1984).
23. Chen, H.-Y., and Sachtler, W. M. H., *Catal. Today* **42**, 73 (1998).
24. Clark, F. T., Springman, M. C., Willcox, D., and Wachs, I. E., *J. Catal.* **139**, 1 (1993).
25. Kung, M. C., and Kung, H. H., *Catal. Rev. Sci. Eng.* **27**, 425 (1985).
26. Topsøe, N. Y., *J. Catal.* **128**, 499 (1991).
27. Belokopytov, Y. V., Kholyavenko, K. M., and Gerei, S. V., *J. Catal.* **60**, 1 (1979).
28. Yamaguchi, T., Jin, T., and Tanabe, K., *J. Phys. Chem.* **90**, 3148 (1986).
29. Yamaguchi, T., *Appl. Catal.* **61**, 1 (1990).
30. Kosaki, Y., Miyamoto, A., and Murakami, Y., *Bull. Chem. Soc. Japan* **52**, 617 (1979).
31. Baes, C. F., Jr., and Mesmer, R. E., *in* "The Hydrolysis of Cations." Wiley, New York, 1976.

32. Kukkadapu, R. K., and Kevan, L., *J. Phys. Chem*. **93**, 1654 (1989).
33. Bahranowski, K., Janas, J., Machej, T., Serwicka, E. M., and Vartikian, L. A., *Clay Miner.* **32**, 665 (1997).
34. Eng, J., and Bartholomew, C. H., *J. Catal.* **171**, 27 (1997).
35. Ramis, G., Yi, L., Busca, G., Turco, M., Kotur, E., and Willey, R. J., *J. Catal*. **157**, 523 (1995).
36. Went, G. T., Leu, L.-J., Rosin, R. R., and Bell, A. T., *J. Catal.* **134**, 492 (1992).
37. Ozkan, U. S., Cai, Y., and Kumthekar, M. W., *J. Phys. Chem*. **99**, 2363 (1995).
38. Odriozola, J. A., Heinemann, H., Somorjai, G. A., Garcia de la Banda, J. E., and Pereira, P., *J. Catal.* **119**, 71 (1989).
39. Schraml, M., Wokaun, A., and Baiker, A., *J. Catal.* **124**, 86 (1990).
40. Odenbrand, C. U. I., Bahamonde, A., Avila, P., and Blanco, J., *Appl. Catal. B* **5**, 117 (1994).
41. Chen, J. P., and Yang, R. T., *J. Catal.* **139**, 277 (1993).
42. He, M. Y., Liu, Z., and Min, E., *Catal. Today* **2**, 321 (1988).
43. Ito, E., Mergler, Y. J., Nieuwenhuys, B. E., Calis, H. P. A., van Bekkum, H., and van den Bleek, C. M., *J. Chem. Soc. Faraday Trans.* **92**, 1799 (1996).
44. Topsøe, N. Y., Slabiak, T., Clausen, B. S., Srnak, T. Z., and Dumesic, J. A., *J. Catal.* **134**, 742 (1992).
45. Ma, A.-Z., and Grunert, W., *Chem. Commun.*, 71 (1999).
46. Long, R. Q., and Yang, R. T., *J. Am. Chem. Soc.* **121**, 5595 (1999).